

# RSC Advances



This is an *Accepted Manuscript*, which has been through the Royal Society of Chemistry peer review process and has been accepted for publication.

*Accepted Manuscripts* are published online shortly after acceptance, before technical editing, formatting and proof reading. Using this free service, authors can make their results available to the community, in citable form, before we publish the edited article. This *Accepted Manuscript* will be replaced by the edited, formatted and paginated article as soon as this is available.

You can find more information about *Accepted Manuscripts* in the [Information for Authors](#).

Please note that technical editing may introduce minor changes to the text and/or graphics, which may alter content. The journal's standard [Terms & Conditions](#) and the [Ethical guidelines](#) still apply. In no event shall the Royal Society of Chemistry be held responsible for any errors or omissions in this *Accepted Manuscript* or any consequences arising from the use of any information it contains.

## ARTICLE

# A Highly Sensitive Gold Nanoparticle Bioprobe Based Electrochemical Immunosensor Using Screen Printed Graphene Biochip

Cite this: DOI: 10.1039/x0xx00000x

Syazana Abdullah Lim<sup>1,3</sup>, Hiroyuki Yoshikawa<sup>2</sup>, Eiichi Tamiya<sup>2</sup>, Hartini Mohd Yasin<sup>3</sup> and Minhaz Uddin Ahmed<sup>3\*</sup>Received 00th January 2012,  
Accepted 00th January 2012

DOI: 10.1039/x0xx00000x

[www.rsc.org/](http://www.rsc.org/)

This study describes a highly sensitive electrochemical immunosensor for the detection of human chorionic gonadotropin (hCG) that uses gold nanoparticle (AuNP) as electrochemical label and graphene as electrode material. Primary antibody was first immobilized on the graphene working electrode surface by physical adsorption. Antigen hCG was then added and sandwiched with a secondary antibody labelled with AuNPs. After this series of sandwich-type immunoreaction was performed on the electrode, AuNPs were quantified by subjecting the immunocomplex to a preoxidation process of high potential at 1.2 V for 40 s and immediately reduced and scanned by differential pulse voltammetry (DPV). Electrodeposition of gold during the reduction stage of the redox reaction was determined by cyclic voltammetry (CV) that showed a linear relationship with the different hCG concentrations. In this study, a linear relationship between reduction peak current signals and hCG concentration from 0 to 500 pg/mL (correlation coefficient of 0.97351) with detection limit of 5 pg/mL was obtained.

## Introduction

Electrochemical devices are the most used sensing elements in biosensors development due to inherent miniaturization, their high sensitivity, low cost and their compatibility with advanced microfabrication technology<sup>1-3</sup>. Analytical work of immunosensors is based on the principle that stable complex forms as a result of specific molecular recognition by antibodies of antigens<sup>4</sup>. The binding of an antigen to its specific antibody is identified and quantitated by coupling the immunochemical reaction to the surface of a transducer. Electrochemical immunosensors have gained momentum across the globe in the research and development department of various areas such as agriculture, food safety, medical diagnostics, quality control, environmental and industrial monitoring<sup>5</sup>, to name a few.

Human chorionic gonadotropin (hCG) is a glycoprotein hormone made up of an  $\alpha$ -subunit and a  $\beta$ -subunit joined together by hydrophobic and ionic noncovalent interactions. While the  $\alpha$ -subunit can also be found in other glycoprotein hormones such as luteinizing hormone, follicle stimulating hormone, and thyroid stimulating hormone, the  $\beta$ -subunit is unique to hCG.

Hydatidiform moles and choriocarcinoma cells produce  $\beta$ -subunit in excess and consequently these are secreted as free  $\beta$ -subunit. The free  $\beta$ -subunit may be used as cancer biomarker as it acts as an autocrine in cancer cells, promotes cell growth, invasion, and metastases<sup>6,7</sup>. Having closely linked to gestational trophoblastic disease, germ cell tumours, non-trophoblastic gynaecological cancers and common epithelial tumours, observing hCG levels in blood serum and urine is essential to cancer monitoring and relapse detection in patients<sup>8</sup>.

Graphene is a two-dimensional planar sheet of  $sp^2$  bonded carbon atoms that are tightly packed in a honeycomb lattice structure<sup>9</sup>. Graphene forms a basis for other carbon allotropes such as single-walled carbon nanotube that could be envisioned as a single graphene sheet wrapped around to form a cylinder whereas multi-walled carbon nanotube consists of multiple layers of graphene sheets rolled to form a cylinder<sup>10</sup>. Graphene possess extraordinary properties for instance, double surface area than that of single walled carbon nanotubes, ultra-high mechanical strength, a tunable electronic band gap, excellent thermal conductivity, room-temperature Hall effect, and ultra-high elasticity<sup>11</sup>. These excellent features are attributed to  $sp^2$  bonds and electron configuration of graphene that makes it an ideal material for potential electronic and electrochemical sensing applications<sup>12</sup>.

The use of highly sensitive tags are imperative in immunosensor work to amplify signal response and lower the detection limits. Metal nano-size tags are shown to be more advantageous in comparison to traditional enzymatic and organic fluorescent dye signal tags as single nano-size tag contains large number of signal molecules thus emitting much higher signal than the conventional single tag containing only one or several signal molecules<sup>13</sup>.

<sup>1</sup>Environmental and Life Sciences Programme, Faculty of Science, Universiti Brunei Darussalam, Jalan Tungku Link, Gadong, BE 1410, Brunei Darussalam,

<sup>2</sup>Nanobioengineering Laboratory, Department of Applied Physics, Graduate School of Engineering, Osaka University, 2-1 Yamada-oka, Suita, Osaka 565-0871, Japan.

<sup>3</sup>Biosensors and Biotechnology Laboratory, Chemical Science Programme, Faculty of Science, Universiti Brunei Darussalam, Jalan Tungku Link, Gadong, BE 1410, Brunei Darussalam. Corresponding Author: Dr. Minhaz Uddin Ahmed, Phone: +673 888 4752. \*Email: minhaz.ahmed@ubd.edu.bn, minhazua@gmail.com

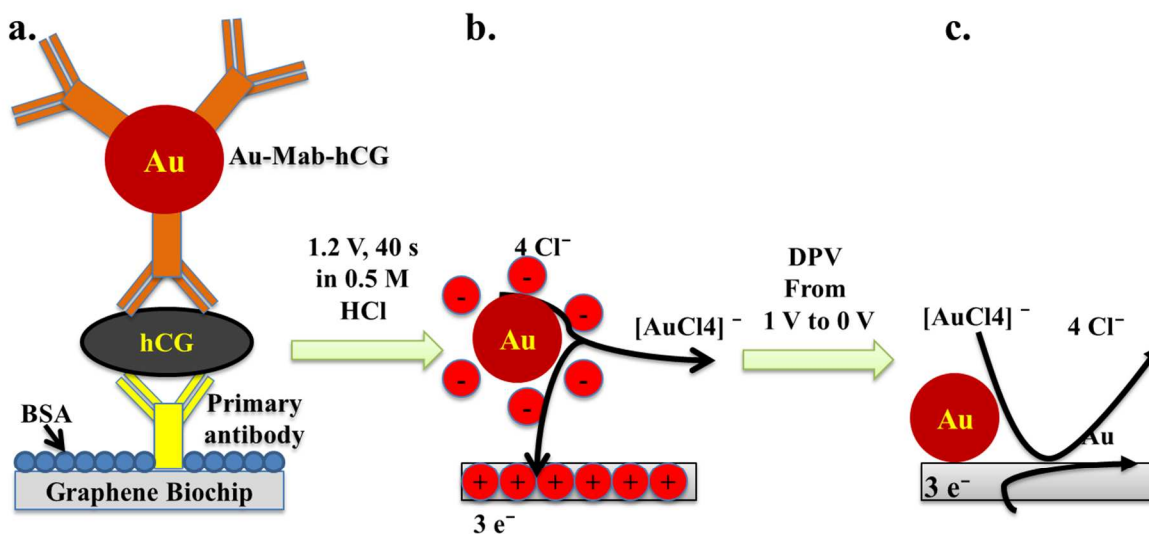


Figure 1. Schematic illustration of the electrochemical immunosensor system. (a) The primary antibody was immobilized onto the graphene working electrode by physical adsorption. Bovine serum albumin (BSA) was applied to block uncoated surface of the electrode. A sandwich-type immunoreaction was then performed. (b) Redox reaction was carried out at a high potential of 1.2 V for 40 s (termed as preoxidation) in 0.5 M HCl to oxidize the AuNPs which were immediately reduced and (c) scanned by DPV from 1 V to 0 V.

Particularly, gold nanoparticles (AuNPs) have gained immense attention from researchers due to their unique characteristics owing to the remarkable electronic configuration, high ratio of surface atoms to bulk atoms, strong localised surface plasmon resonance band that allows electromagnetic confinement through interaction with optical wave, quantum effects and other traits resulting from their extremely small sizes<sup>14</sup>. AuNPs are also mostly used as signal probe owing to their ease of fabrication and functionalization, and high stability<sup>15-17</sup>. An example of using nanoparticles to load large amount of signal molecules was a study by Omidfar *et al.*<sup>18</sup>. Upon conjugation of AuNPs with anti-human serum albumin (HSA), a competitive immunoreaction was performed. Then, oxidation of AuNPs was carried out in 0.1 M HCl at high potential of 1.3 V for 80 s followed by reduction of  $\text{AuCl}_4^-$  to  $\text{Au}^0$  in differential pulse voltammetry (DPV) mode to produce the electrochemical signals. This approach is based on the oxidoreduction properties of the AuNPs in acidic medium where target analyte in sample is detected through the quantification of nanoparticles. A decrease in DPV responses was observed with increasing concentrations of HSA in standard and real samples. In optimal conditions, this immunosensor based on MCM-41-PVA nanocomposite film could detect HSA in a high linear range (0.5–200 ng/mL) with a low detection limit of 1 ng/mL. Lai *et al.*<sup>19</sup> based their work on the principle of utilizing nanoparticles to induce deposition of metal for further amplification with streptavidin-functionalized silver-nanoparticle-enriched carbon nanotube (CNT/Ag NP) served as trace label for sensitive detection of carcinoembryonic antigen (CEA) and  $\alpha$ -fetoprotein (AFP). This group chose silver nanoparticles (AgNPs) in their investigation as these nanoparticles can be oxidized at more negative potential with a relatively sharp peak thus eliminating the interference of reducing species and improving the detection precision and sensitivity. Through a sandwich-type immunoreaction on the immunosensor array, numerous AgNPs are captured onto every single immunocomplex and are further amplified by a subsequent AgNP-promoted deposition of silver from a silver enhancer solution to obtain the sensitive electrochemical-stripping signal of the AgNPs. The amplified Ag NPs showed well-defined anodic stripping peak in 1.0 M KCl solution. Both the high content of AgNPs on the

synthesized tag and the following silver enhancement greatly amplified the detection signal, which led to a detection limit down to 0.093 and 0.061 pg/mL for CEA and AFP respectively. However, this procedure suffered from the disadvantages of complicated fabrication and instability of AgNP probe. To circumvent these problems, another group<sup>17</sup> used gold nanoparticles (AuNPs) synthesized *in situ* to catalyze the deposition of silver labeled to the signal antibody. They designed a triple signal amplification strategy combining the AuNPs-catalyzed Ag deposition after sandwich-type immunoreaction to amplify the anodic stripping signal with graphene for rapid electron transfer and microbead carried AuNPs. The triple signal amplification greatly enhanced the sensitivity for CEA detection with a linear range of 0.5 pg/mL to 0.5 ng/mL and a detection limit down to 0.12 pg/mL.

The outstanding signal enhancement potential of AuNPs and their ability to form bioconjugated molecules, together with the remarkable sensitivity of graphene, have become the basis of this study to design a highly sensitive electrochemical biosensor. Our signal amplification strategy involved physical immobilization of primary antibody onto disposal graphene-modified screen-printed carbon electrode (SPCE) or graphene biochip. Antigen hCG was then added and sandwiched with a secondary antibody labelled with AuNPs. This was then subjected to a high potential of 1.2 V for 40 s in 0.5 M HCl and immediately followed by voltammetric measurement (Figure 1).

## Materials and Methods

### Reagents and Materials

Monoclonal anti-human  $\alpha$ -subunit of follicle-stimulating hormone (Mab-FSH) and monoclonal anti-human chorionic gonadotropin (Mab-hCG), with affinity constants of  $2.4 \times 10^9 \text{ M}^{-1}$  and  $4.4 \times 10^9 \text{ M}^{-1}$  respectively, were obtained from Medix Biochemica (Finland). The molecular weight hCG (Abdserotec, UK) was stated to be 39.5 kD by SDS PAGE. Colloidal solution of Au nanoparticles with diameter of 40 nm of optical density 10 was purchased from BBI solutions (UK).

Bovine serum albumin (BSA), sodium azide ( $\text{NaN}_3$ ), HCl,  $\text{Na}_2\text{HPO}_4$ ,  $\text{NaH}_2\text{PO}_4 \cdot 2\text{H}_2\text{O}$ , polyethylene glycol (PEG), and  $\text{KH}_2\text{PO}_4$  were purchased from Sigma-Aldrich (USA). All solutions were prepared and diluted using double distilled water.

### Instrumentations

Cyclic voltammetry (CV) and Differential Pulse Voltammetry (DPV) were performed using a Autolab PGSTAT101 III (Metrohm, Netherlands) working together with its Nova 1.10 software. The screen-printed electrodes (SPEs) were purchased from DropSens (Spain) and consisted of a graphene modified working electrode, a carbon counter-electrode, and silver reference electrode. All measurements were made at room temperature ( $21 \pm 1^\circ\text{C}$ ).

### Preparation of graphene biochip

Immobilization of primary antibody was carried out by dropping 6.68  $\mu\text{L}$  of Mab-FSH solution (100  $\mu\text{g}/\text{mL}$  in 50 mM phosphate buffered saline (PBS, pH 7.4) onto the surface of working electrode and incubated overnight at  $4^\circ\text{C}$ . After incubation, excess antibodies were rinsed with PBS. Following rinsing, 50  $\mu\text{L}$  of blocking solution (1% BSA in PBS) was added onto the electrode surface to prevent non-specific binding and incubated at  $4^\circ\text{C}$  for another 12 h. The blocking solution was then washed with PBS. The Mab-FSH-immobilized immunosensor was stored at  $4^\circ\text{C}$  until needed.

### Bioconjugation of gold nanoparticle to hCG antibody (Au-Mab-hCG)

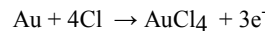
A mixture of 100  $\mu\text{L}$  of Mab-hCG solution (50  $\mu\text{g}/\text{mL}$  in 5 mM  $\text{KH}_2\text{PO}_4$ , pH 7.5) and 900  $\mu\text{L}$  of 0.1% Au nanoparticle solution was prepared and kept for 10 min at room temperature. To block any uncovered surface on the AuNPs, 50  $\mu\text{L}$  of 1% PEG in 50 mM  $\text{KH}_2\text{PO}_4$  solution (pH 7.5) and 100  $\mu\text{L}$  of 10% BSA in 50 mM  $\text{KH}_2\text{PO}_4$  solution (pH 9.0) were added. The Au nanoparticle-conjugated Mab-hCG (Au-Mab-hCG) was then collected through centrifugation (8000 g for 15 min at  $4^\circ\text{C}$ ). Au-Mab-hCGs were suspended in 1 mL of preservation solution (1% BSA, 0.05% PEG 20000, 0.1%  $\text{NaN}_3$  and 150 mM NaCl in 20 mM Tris-HCl buffer, pH 8.2), and centrifuged again to collect the Au-Mab-hCGs. Au-Mab-hCGs were then suspended in the preservation solution and stored as stock solution.

### Sandwiched immunocomplex reaction procedure

Antigen hCG was prepared at various concentrations (between 0 and 500  $\text{pg}/\text{mL}$ ) with 1% BSA in PBS. Then, 6.68  $\mu\text{L}$  of these antigen hCG solutions were added onto the Mab-FSH-immobilized immunosensor and left to incubate for 30 min at room temperature with moderate shaking allowing for the antigen-antibody reaction. Au-Mab-hCG stock solution was diluted to 10-fold and 6.68  $\mu\text{L}$  of this diluted solution was applied onto the rinsed surface. After incubation for another 30 min at room temperature, the surface was washed with blank PBS.

### Preoxidation of AuNPs and signal measurement

A direct redox reaction was carried out using 50  $\mu\text{L}$  of 0.5 M HCl covering the entire three-electrode zone of the SPE at room temperature. The analytical procedure was based on the following process on the electrode surface: the preoxidation of the colloidal gold was performed at constant potential of 1.2 V for 40 s producing  $\text{AuCl}_4^-$  ions absorbed on graphene electrode surface:



$\text{AuCl}_4^-$  ions were immediately reduced<sup>20</sup> to Au at 0.35 V and the reduced ions were scanned in the potential range from 1 V to 0 V with a step potential of 4 mV, a modulation amplitude of -50 mV, a modulation time of 50s and an interval time of 200 ms. The potentials were obtained against the Ag/AgCl reference electrode printed within the SPE.

## Results and Discussion

### Mab-AuNP conjugation characterization

Conjugation of antibody to AuNP was confirmed by UV-Vis measurements because AuNPs and protein have different absorbance wavelength of  $A_{525}$  and  $A_{280}$  respectively<sup>21</sup>. Prior to the addition of antibody, the absorption value of colloidal gold was observed at 528 nm. After addition of antibody, bonds were formed between AuNPs and the amino groups of the antibody causing the absorbance maximum value shifted to 550 nm due to a change in refractive index as a consequence of the attachment of antibody layer on AuNPs thus confirming the antibody conjugation to gold<sup>22</sup>.

### Electrochemical Characterization of Immunosensor

To investigate the reduction properties of Au ions to Au in HCl, comparison work was carried out between carbon SPE and graphene-modified SPCE. Figure 2 displays CV graphs of bare and AuNPs-incubated graphene (graph A) and carbon (graph B) electrodes in the potential range from -0.8V to 1.3 V. The reduction signal of AuNPs for both electrodes could be observed at the potential of 0.36 V. By comparing the current signals for both electrodes, it was revealed that graphene (curve 2A (b)) exhibited a more prominent reduction peak (19  $\mu\text{A}$ ) as compared to carbon (curve 2B (d) with reduction peak of 1.7 $\mu\text{A}$ ). This demonstrated that graphene promotes the reduction of AuNPs better than carbon due to not only the high surface area of graphene but also its outstanding electron transfer attribute<sup>23</sup>. Kampouris and Banks<sup>24</sup> reported that enhanced electron transfer of graphene occur primarily at the edge of the graphene rather than at the basal.

## ARTICLE

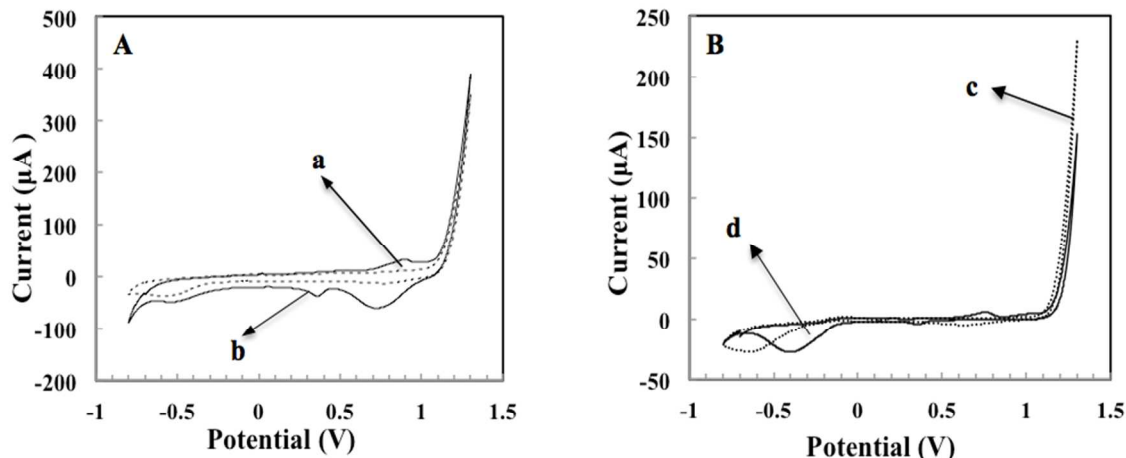


Figure 2. The cyclic voltammograms of bare (a) and AuNPs immobilised (b) on graphene SPE (A) electrode at 100 mV/s in 0.5 M HCl. The cyclic voltammograms of bare (c) and AuNPs immobilised (d) on SPCE (B) at 100 mV/s in 0.5 M HCl.

DPV graphs presented in Figure 3 are obtained from Au-Mab-hCG immobilised immunosensor with hCG concentrations varying from 0 to 500 pg/mL in PBS. The reduction signal was observed at 0.35 V and the peak current intensified in correlation with the increasing hCG concentrations.

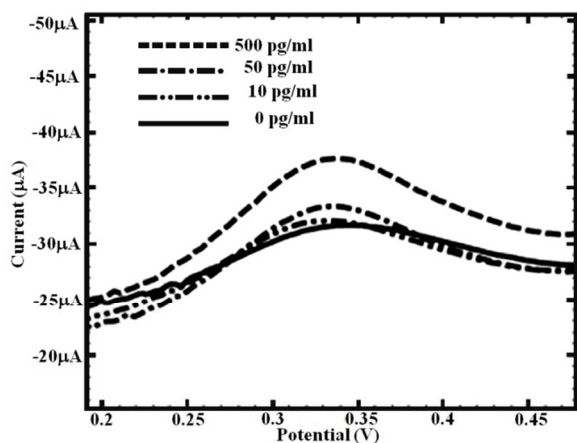


Figure 3. DPV of the Au-Mab-hCG on graphene electrodes.

The formation of different layers on the working graphene electrode surface was characterized by CV using  $\text{Fe}(\text{CN})_6^{3-}/\text{Fe}(\text{CN})_6^{4-}$  as a redox probe after each assembly step. As shown in Figure 4, cyclic voltammogram on the bare and Au-Mab-hCG immobilized SPEs were obtained with a reversible redox peak of 10 mM  $\text{Fe}(\text{CN})_6^{3-}/\text{Fe}(\text{CN})_6^{4-}$  with oxidation and reduction peaks of bare electrode observed at 0.2 V and 0 V respectively (curve a). Upon immobilization of primary antibody (Mab-FSH) on the electrode surface, an insulating layer was formed in which redox

probe could not reach and this subsequently decreased rate of current transfer (curve b)<sup>25</sup>. After adding antigen hCG (curve c) and Au-Mab-hCG (curve d), interestingly no further significant decrease in redox peaks were seen. This could be due to protein fouling caused by the immobilized antibody molecules and/or at pH values greater than the isoelectric point of antibody, electrostatic interactions between the anionic  $\text{Fe}(\text{CN})_6^{3-}/\text{Fe}(\text{CN})_6^{4-}$  and the negatively charged antibody molecules could occur<sup>26</sup>. Then, after redox electrochemical reactions of various concentrations of hCG in 0.5 M HCl were performed, the response current in  $\text{Fe}(\text{CN})_6^{3-}/\text{Fe}(\text{CN})_6^{4-}$  significantly decreased (curve e). The decrease in current response was due to a layer of Au being electrodeposited on the graphene electrode when Au ions were reduced during the redox reaction process in HCl<sup>27</sup> that further hinder electrons reaching the electrode surface.

In order to establish the relationship upon electrochemical redox reaction of different hCG concentrations in 0.5 M HCl and oxidation peak current signals measured in 10 mM  $\text{Fe}(\text{CN})_6^{3-}/\text{Fe}(\text{CN})_6^{4-}$  solution, a calibration graph was plotted. As shown in Figure 5, the oxidation peak current response of 10 mM  $\text{Fe}(\text{CN})_6^{3-}/\text{Fe}(\text{CN})_6^{4-}$  solution depended linearly on the concentration of hCG hormone with correlation coefficient of 0.9974 with linear range from 50 to 1000 pg/mL. This phenomenon was due to the layering of Au that was produced when Au ions were reduced to form Au. This result also served as evidence that at higher hCG concentrations more attachment of Mab-hCG-AuNPs to hCG occurred and more formation of antigen-antibody-AuNPs complexes which subsequently deposit thicker layer of Au onto the graphene electrode surface after electrochemical redox process in 0.5 M HCl. This led to lower current signal as Au acts as a barrier that impedes electron transfer between the redox probe and the electrode surface.

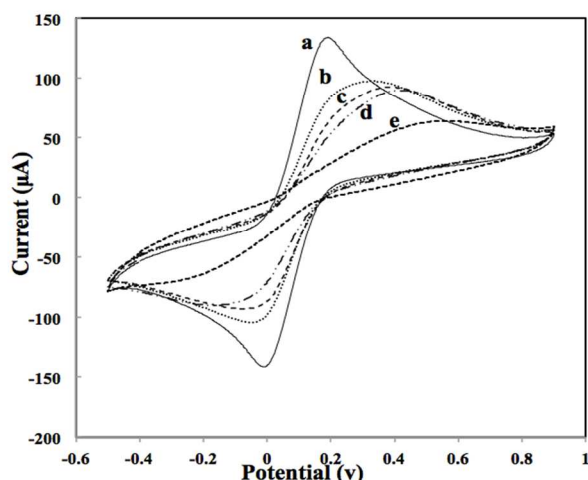


Figure 4. Cyclic voltammograms of 10 mM  $\text{Fe}(\text{CN})_6^{3-}/\text{Fe}(\text{CN})_6^{4-}$  solution in 50 mM phosphate buffer (pH 7) at (a) a bare graphene electrode, (b) Mab-FSH-modified graphene electrode, (c) after adding antigen hCG hormone, (d) after adding Au-Mab-hCG and (e) after electrochemical redox reaction of 1000 pg/mL hCG hormone in 0.5 M HCl. Potential range from -0.5 to 0.9 V with scan rate of 100 mV/s.

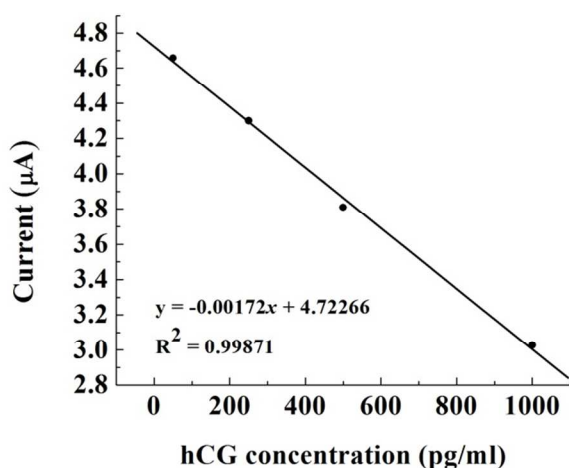


Figure 5. Calibration plots that illustrate the relationship between the hCG concentrations (after redox reaction in 0.5 M HCl) and the oxidation peak current signals measured in 10 mM  $\text{Fe}(\text{CN})_6^{3-}/\text{Fe}(\text{CN})_6^{4-}$  solution in 50 mM phosphate buffer pH 7. The limit of detection of 50 pg/mL of hCG was obtained.

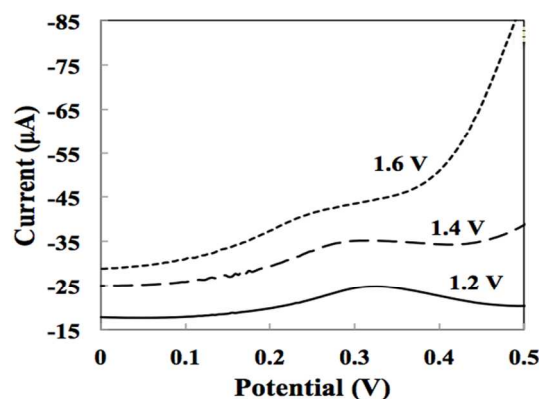


Figure 6. DPV graphs of Au-Mab-hCG on graphene modified SPCE in 0.5 M HCl at hCG concentration of 250 pg/mL. Different pre-oxidation potentials (1.20 V, 1.40 V and 1.60 V) were used after the immunocomplexes formation with pre-oxidation time set at 40 s.

### Electrochemical Optimization of the Immunosensor

The preoxidation potential was optimized in this study by assigning potentials of 1.20, 1.40 and 1.60 V vs Ag/AgCl with a pre-oxidation time of 40 s using 250 pg/mL of hCG and the respective reduction peak current responses were investigated. Figure 6 shows that increasing the pre-oxidation potential has resulted in decreasing reduction peak current intensity which suggested more Au ions are lost at higher pre-oxidation potential<sup>28</sup>. Maximum reduction peak was discerned at 1.20 V with peak disappearing at 1.40 V. Hence, 1.20 V was chosen to be the optimum pre-oxidation potential used throughout this study.

### Analytical Performance of Electrochemical System

The principle of our detection system was based on the peak current intensities of Au ions reduced in 0.5M HCl by DPV. Different concentrations of hCG ranging from 0 to 500 pg/mL was used to evaluate the analytical linear range and sensitivity of our immunosensor. Increasing the hCG concentrations also enhance the intensity of reduction peak current responses with correlation coefficient found to be 0.97351 (Figure 7). This correlation coefficient value obtained in the DPV was attributed to the irreproducible deposition of Au onto the graphene biochips. In addition, DPV is more sensitive and gives higher resolution when compared to CV. A detection limit of 5 pg/mL was achieved for hCG under the optimum conditions.

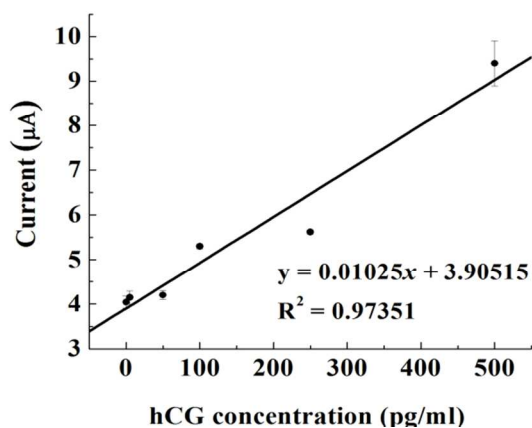


Figure 7. Calibration curve for the detection of hCG established from peak current intensities of AuNPs.

### Comparison of different studies for hCG detection using SPE

A comparison to determine hCG hormones using this method with different electrode materials published by other groups is displayed in Table 1. By far, our group achieved a lower detection limit by using graphene biochip in AuNPs redox in HCl signal amplification approach than the work by Idegami<sup>27</sup> and Xuan Viet<sup>28</sup> groups that used carbon SPE and single-walled carbon nanotube-modified carbon SPE which were reported to be 36 pg/mL and 13 pg/mL respectively for the detection of hCG. It is important to highlight that the SPE used in this study comprised of inert carbon counter electrode that is advantageous over platinum counter electrodes. In acidic solution, platinum dissolved and formed platinum ions which may affect the activity of reaction on the working solution<sup>29</sup>. The lower detection limit in our work might be associated to, as discussed earlier, the large surface area and outstanding electron transfer performance of graphene due to the presence of more sp<sup>2</sup>-like planes and various edge defects present on its surface<sup>30</sup>. Lu *et al.*<sup>31</sup> and Yang *et al.*<sup>32</sup> demonstrated the superiority of graphene as a sensing material in similar studies but employing the catalytic reaction of hydrogen peroxidase towards the reduction of hydrogen peroxide where they achieved low detection limits of 2.6 pg/mL for the detection of hCG and 50 pg/mL for human IgG respectively.

Table 1. Comparison of different studies for the determination of hCG hormone using SPCEs.

Methods	Working electrode	Limit of detection	Reference
DPV	SPCE	36 pg/ml	27
DPV	Single walled carbon nanotube-modified SPCE	13 pg/ml	28
DPV	Graphene-modified SPCE	5 pg/ml	This work

### Conclusions

The combined merits of AuNPs and graphene were explored in this study. To the best of our knowledge, this is the first study that uses graphene-modified carbon SPEs or graphene biochip for the detection of hCG using AuNPs redox in HCl signal enhancement strategy and we have achieved a LOD of 5 pg/mL for the detection of hCG hormone. Our work with graphene produced the best LOD over other SPEs and this paves ways for more graphene-related work in our laboratory to detect other cancer biomarkers in the future.

### Acknowledgement

S.A. Lim would like to thank the Ministry of Education, Brunei Darussalam for the opportunity given to undertake a Ph.D programme at Universiti Brunei Darussalam (UBD). The authors also acknowledge Nur Syakimah Ismail from Department of Applied Physics, Graduate School of Engineering, Osaka University and Kisan Koirala from Chemical Science Programme, Faculty of Science, UBD for their kind assistance and helpful discussion in this work.

### References

- 1 D.R.Thévenot., K. Toth, R.A. Durst, G.S. Wilson, *Pure Appl Chem*, 1999, **71**, 2333–2348.
- 2 M. U. Ahmed, I. A. Saaem, P. C. Wu, A. Brown, *Critical Review in Biotechnology*, 2014, **34**, 180-196.
- 3 M.U. Ahmed, M.M. Hossain, E. Tamiya, *Electroanalysis*, 2008, **20**, 616-626.
- 4 R.P. Ekins, *J. Clin. Ligand Assay*, 1999, **22**, 61-77.
- 5 S. Ripp, M.L. Diclaudio and G.S. Sayler, "Chapter 9: Biosensors as Environmental Monitors" in *Environmental Microbiology, Second Edition*, edited by Ralph Mitchell and Ji-Dong Gu, Wiley-Blackwell, 2010.
- 6 K.Visconti and N. Zite, *Clinical Obstetrics and Gynecology*, 2012, **55**, 410-417.
- 7 L.A. Cole, *Placenta*, 2007, **28**, 977-986.
- 8 P.Kassanos, R.K. Iles, R.H. Bayford and A. Demosthenous, *13th International Conference on Electrical Bioimpedance and the 8th Conference on Electrical Impedance Tomography*, IFMBE Proceedings, 2007, **17**, 620 – 623.
- 9 Y.C. Lin and P.W. Chiu, in *Graphene: Properties, Preparation, Characterisation and Devices*, Edited by: V .Skakalova and A. Kaiser, 2014, 265-291.
- 10 K. Dasgupta, J.B. Joshi and S. Banerje, *Chemical Engineering Journal*, 2011, **171**, 841–869.

- 11 A.K. Geim, *Science*, 2009, **324**, 1530-1534.
- 12 D. Chen, L.H. Tang and J.H. Li, *Chemical Society Review*, 2010, **39**, 3157-3180.
- 13 J.U. HuangXian, *Science China Chemistry*, 2011, **54**, 1202–1217
- 14 C. Louis and O. Pluchery, *Gold nanoparticles for physics, chemistry and Biology*. World Scientific Publisher, 2012. ISBN: 978-1-84816-806-0.
- 15 L. Ding, A.M. Bond, J. Zhai, J. Zhang, *Analytica Chimica Acta*, 2013, **797**, 1-12.
- 16 V.K.K. Upadhyayula, *Analytica Chimica Acta*, 2012, **715**, 1–18
- 17 D.Lin, J. Wu, M. Wang, F. Yan and H.Ju. *Anal. Chem.*, 2012, **84**, 3662–3668.
- 18 Omidfar K, Zarei H, Gholizadeh F, Larijani B. *Analytical Biochemistry*, 2012, **421**,649–656
- 19 G. Lai, J. Wu, H. Ju, F. Yan, *Advanced Functional Materials*. 2011, **21**, 2938-2943.
- 20 Z.P. Chen, Z.F. Peng, P. Zhang, X.F. Jin, J.H. Jiang, X.B. Zhang, G.L. Shen and R.Q. Yu, *Talanta*, 2007, **72**, 1800–1804.
- 21 J.W. Choi, D.Y. Kang, Y.H. Jang, H.H. Kim, J Min, B.K. Oh, *Colloids and Surfaces A: Physicochemical and Engineering Aspects*, 2008, **313-314**, 655-659
- 22 S.Thobhani, S. Attree, R.Boyd, N. Kumarswami, J.N.M.Szymanski, R.A. Porter, *Journal of Immunological Methods*, 2010, **356**, 60-69
- 23 Y.Fang and E.Wang, Electrochemical Biosensors on Platforms of Graphene, *Chem. Commun.*, 2013, 49, 9526
- 24 D.K. Kampouris and C.E. Banks, *Chem. Commun.*, 2010, **46**, 8986–8988
- 25 Q. Li, N. Li, P. Le Tissier, Grattan D.R., K. Kerman, *Electroanalysis*, 2012, **24**, 1272-1276.
- 26 J.A. Ho, H.C. Chang, N.Y. Shih, L.C. Wu, Y.F.Chang, C.C. Chen and C.Chou, *Analytical Chemistry*, 2010, **82**, 5944-5950.
- 27 K. Idegami, M. Chikae, K. Kerman, N. Nagatani, T. Yuhi, T.Endo and E. Tamiya, *Electroanalysis*, 2008, **20**,14-21.
- 28 N. Xuan Viet, M. Chikae, Y. Ukita, K. Maehashi, K. Matsumoto, E. Tamiya, P. Hung Viet and Y. Takamura, *Biosensors and Bioelectronics*, 2013, **42**, 592-597.
- 29 C.Gu, B.C. Norrris, F.R.F. Fan, C.W. Bielawski, and A.J. Bard, *ASC Catalysis*, 2012, **2**, 746–750.
- 30 S.Alwarappan, A.Erdem, C.Liu and C.Z. Li, *J. Phys. Chem. C.*, 2009, **113**, 8853.
- 31 J Lu, S Liu, S Ge, M. Yan, J.Yu and X. Hu, *Biosensors and Bioelectronics*, 2012, **33**, 29-35.
- 32 Y.C. Yang, S.W. Dong, T. Shen, C.X. Jian, H.J.Chang, Y. Li, J.X. Zhou, *Electrochimica Acta*, 2011, **56**, 6021–6025.